Journal of Medicinal Chemistry

Brief Article

pubs.acs.org/jmc

Design, Synthesis, and Biological Evaluation of Conformationally Constrained Analogues of Naphthol AS-E as Inhibitors of CREB-Mediated Gene Transcription

Min Jiang,[†,‡] Bingbing X. Li,[†,‡] Fuchun Xie,[†,‡] Frances Delaney,[†,‡] and Xiangshu Xiao*[,†,‡,§]

[†]Program in Chemical Biology, [‡]Department of Physiology and Pharmacology, and [§]Knight Cancer Institute, Oregon Health & Science University, 3181 SW Sam Jackson Park Road, Portland, Oregon, United States

Supporting Information

ABSTRACT: Cyclic AMP response element binding protein (CREB) is often dysregulated in cancer cells and is an attractive cancer drug target. Previously, we described naphthol AS-E (**1**) as a small molecule inhibitor of CREB-mediated gene transcription. To understand its bioactive conformation, a series of conformationally constrained analogues of **1** were designed and synthesized. Biological evaluation of these analogues suggests that the global energy minimum of **1** is the likely bioactive conformation.

INTRODUCTION

Cyclic-AMP response element (CRE) binding protein (CREB) is a stimulus-activated nuclear transcription factor enabling cells to respond to various extracellular stimuli.[1] Its DNA-binding domain, located at the C-terminus, binds the consensus CRE sequence 5′-TGACGTCA-3′.[2,3] Even though CREB is able to bind CRE in the absence of any posttranslational modifications, its transcription activity is not activated until its activation domain called kinase-inducible domain (KID) is phosphorylated at Ser133.[4] The thus phosphorylated CREB (p-CREB) allows for its subsequent binding with transcription coactivator CBP (CREB-binding protein).[5] The CREB−CBP interaction is mediated by KID in CREB and KIX (KID-interacting) domain in CBP.[5] A variety of protein serine/threonine kinases including protein kinase A (PKA),[2] protein kinase B (PKB/Akt),[6] protein p90 ribosomal S6 kinase ($pp90^{RSK}$),[7] and mitogen-activated protein kinase (MAPK)[8,9] could phosphorylate and activate CREB. Since these kinase signaling pathways are often deregulated in cancer cells, CREB was consistently found to be overactivated in cancer tissues from patients with non-small-cell lung cancer (NSCLC),[10] prostate cancer,[11] breast cancer,[12] acute myeloid leukemia, and acute lymphoblastic leukemia.[13,14] Thus, CREB has been proposed as an intriguing target for the development of novel cancer therapeutics[15] and various strategies have been pursued to identify potential small molecule modulators of CREB-mediated gene transcription.[15−17]

We recently described naphthol AS-E (**1**, Figure 1) as a small molecule inhibitor of KIX−KID interaction and CREB-mediated gene transcription with potencies in the low micromolar range.[18] However, its bioactive conformation, which would be very useful in facilitating the design of more potent analogues, is currently unknown. In this report, a series of conformationally constrained analogues of **1** were designed and synthesized to interrogate the bioactive conformation of **1** as inhibitors of KIX−KID interaction and CREB-mediated gene transcription.

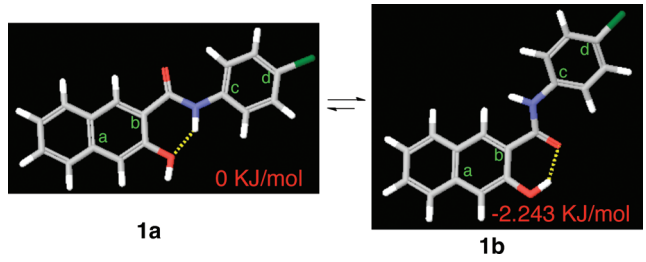

Figure 1. Potential conformations of **1**. The yellow dashed lines indicate hydrogen bonds. The dihedral angle of a−b−c−d in **1a** is 0.1°, while that in **1b** is 10.6°.

RESULTS AND DISCUSSION

To investigate the conformational preference of **1**, it was subjected to a systematic conformational search by rotating all the rotatable bonds in MacroModel. This search resulted in two alternatively hydrogen-bonded conformations **1a** and **1b** (Figure 1) as the energy minima. Conformer **1a**, with a dihedral angle of a−b−c−d of 0.1°, is fully conjugated and adopts a coplanar conformation. On the other hand, the dihedral angle of a−b−c−d in conformer **1b** is 10.6°. As a consequence, the naphthyl ring and the chlorophenyl ring are not coplanar. Counterintuitively, conformer **1b** is the global minimum and is energetically slightly more favorable than conformer **1a** by 2.243 kJ/mol (Figure 1). To examine which conformation might represent the biologically active one, conformationally constrained analogues **2**−**7** (Chart 1) were designed. Compounds **2** and **3** were designed to mimic conformer **1a**, while **4**−**7** were designed to mimic conformer **1b**.

Compound **2** was synthesized in one step by treating **1** with oxalyl chloride.[19] The synthesis of benzo[*g*]quinazolinedione **3** would require precursor **11** (Scheme 1). Therefore, the amino

Received: January 12, 2012
Published: March 29, 2012

dx.doi.org/10.1021/jm300043c | *J. Med. Chem.* 2012, 55, 4020−4024

Chart 1. Structures of Designed Conformationally Constrained Compounds 2−7

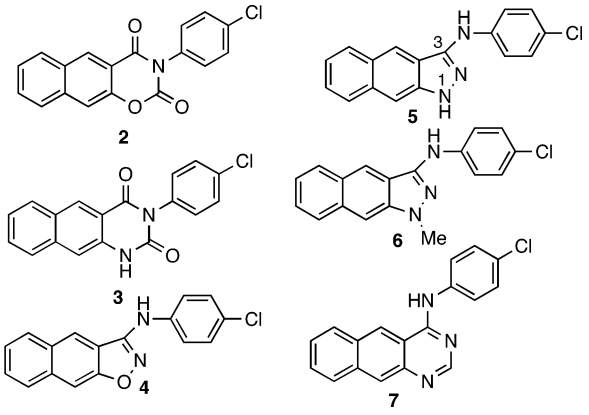

Scheme 1. Synthesis of 3

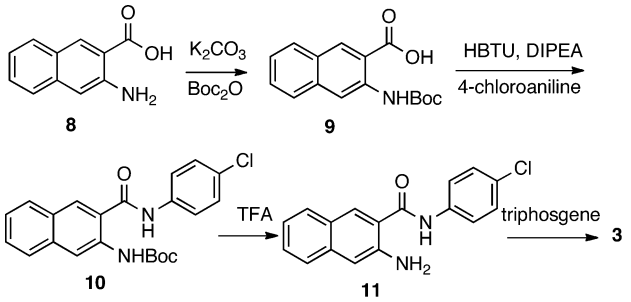

group in 3-amino-2-naphthoic acid (**8**) was first protected by a Boc group to give acid **9**, which was then coupled with 4-chloroaniline to provide amide **10**. Removal of Boc under acidic condition (TFA) yielded amine **11**, which was then treated with triphosgene to afford analogue **3** uneventfully.

The synthesis of analogue **4** was less straightforward. Initially, it was envisioned that an S_NAr reaction between 4-chloroaniline and chloride **15** would deliver **4**.[20] Thus, a synthetic route depicted in Scheme 2 was designed. Hydroxamide **13** was

Scheme 2. Attempted Synthesis of 14

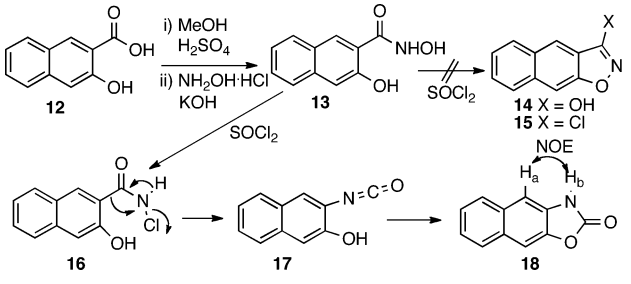

prepared by condensing hydroxylamine with the methyl ester of acid **12**. However, when **13** was treated with thionyl chloride,[21] isoxazole **14** was not obtained as expected. Instead, oxazolone **18** was isolated in 37% yield, whose structure is consistent with the observed positive NOE between H_a and H_b. The formation of **18** is perhaps through a process analogous to the Lossen rearrangement[22] of chloride **16** generated from chlorination of **13** to provide isocyanate **17**, cyclization of which produced **18**. The electron-rich nature of the naphthyl ring may facilitate the Lossen type rearrangement pathway instead of direct ring closure to form **14**. Other reagents including carbonyldiimidazole[23] and Mitsunobu reagent (Ph_3P/DEAD)[24] were also tried, but they both failed to give **14**.

The apparent difficulty in synthesizing **14** prompted us to investigate an alternative route to make **4** as presented in Scheme 3. Thus, 3-amino-2-naphthoic acid (**8**) was converted

Scheme 3. Synthesis of 4−6

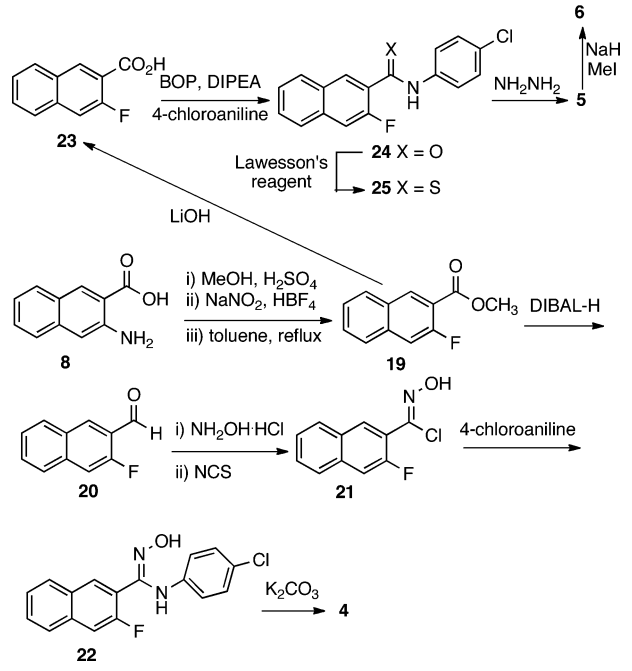

into fluoride **19** through a three-step sequence involving methyl esterification, diazonium salt formation, and thermal decomposition of the diazonium tetrafluoroborate. The ester group in **19** was then reduced with DIBAL-H to provide aldehyde **20**, which was then transformed into the corresponding oxime. It was found that the oxime could be oxidized by NCS to give *N*-hydroxyimidoyl chloride **21**,[25] which was then coupled with 4-chloroaniline to yield *N*-hydroxyimidamide **22**. Intramolecular S_NAr reaction of **22** under basic condition (K_2CO_3/DMF) delivered analogue **4**.

The intermediate ester **19** was also utilized to synthesize **5** and **6** (Scheme 3). Saponification of ester in **19** gave acid **23**, which was then coupled with 4-chloroaniline with BOP reagent to afford amide **24**. The thioamide **25** was formed by treating **24** with Lawesson's reagent. Ring closure between **25** and hydrazine[26] delivered analogue **5**. Methylation of **5** with NaH/MeI afforded **6**. The regiochemistry of the methyl group in **6** was confirmed by the positive NOE between the methyl protons and one of the naphthyl protons, while no NOE was observed between the protons in the chlorophenyl ring and the methyl group.

Finally, **7** was prepared by a sequence of reactions presented in Scheme 4. Intermediate **26** was prepared by condensing acid **8** with formamide under solvent-free conditions.[27] **7** was made by an S_NAr reaction between 4-chloroaniline and chloride **27**, which was derived from **26** after being treated with $POCl_3$.

Compounds **2**−**7** were then evaluated for inhibition of KIX−KID interaction in vitro by a Renilla luciferase complementation assay that we recently developed (Table 1).[18] In this assay, **1** inhibits KIX−KID interaction with IC_{50} = 2.90 μM.[18] **2** and **3** were designed to mimic conformation **1a**. Compound **3** also retains a hydrogen-bond donor as seen in **1**. However, neither

dx.doi.org/10.1021/jm300043c | J. Med. Chem. 2012, 55, 4020−4024

Scheme 4. Synthesis of 7

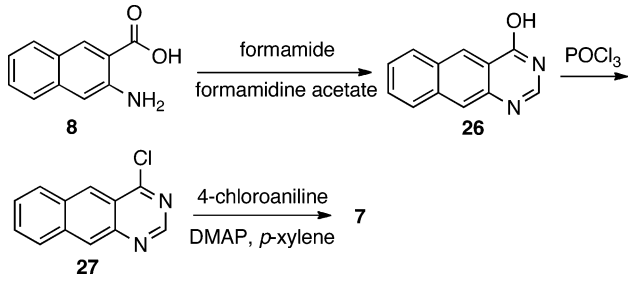

Table 1. Biological Activities of 1−7[a]

compd	KIX−KID inhibition (μM)[b]	CREB inhibition (μM)[c]
1	2.90 ± 0.81	2.29 ± 0.31
2	>50	30.84 ± 8.40
3	>50	>50
4	>50	24.45 ± 16.80
5	8.74 ± 1.68	4.75 ± 3.88
6	5.19 ± 2.20	>50
7	9.46 ± 4.15	18.96 ± 6.09

[a]All the biological activities are presented as IC_{50} with mean ± SD of at least two independent experiments or >50 if IC_{50} was not reached at the highest tested concentration, which is 50 μM. [b]KIX−KID inhibition was evaluated by an in vitro Renilla luciferase complementation assay. [c]CREB inhibition refers to inhibition of CREB-mediated gene transcription in HEK 293T cells using a CREB reporter assay.

of these compounds showed any activity in inhibiting KIX−KID interaction in vitro, suggesting that conformation **1a** may not be biologically relevant. This lack of activity also translates into low or no inhibitory activity against CREB-mediated gene transcription in HEK 293T cells using a CREB reporter assay.[18] Compounds **4**−**7** were designed to interrogate if conformation **1b** is a potential bioactive one. Although **4** was inactive in inhibiting KIX−KID interaction, **5** with a nitrogen linkage showed only slightly reduced activity (IC_{50} = 8.74 μM) compared to **1**. The loss of activity with **4** does not seem to be due to elimination of a hydrogen-bond donor present in **1** because the methylated **6** (IC_{50} = 5.19 μM) and benzo[*g*]-quinazoline **7** (IC_{50} = 9.46 μM) were in the same range of activity as **1**. In the cell-based CREB reporter assay, the oxygen-linked **4** had very weak activity, as expected from its lack of activity in the KIX−KID interaction assay. Compound **5**, on the other hand, retained activity in inhibiting CREB-mediated gene transcription with IC_{50} = 4.75 μM. The intermediate potency of inhibiting KIX−KID interaction by **7** was also reflected in its medium potency in CREB transcription reporter assay (IC_{50} = 18.96 μM). However, the methylated **6** was inactive in cell-based CREB reporter assay even though it was a reasonable inhibitor of KIX−KID interaction. This discrepancy could result from unfavorable cellular permeation and/or subcellular distribution of **6**, which has a higher cLogP (cLogP = 5.298) than **5** (cLogP = 4.433). Taken together, these results suggest that the likely bioactive conformation of **1** resembles conformer **1b**.

To further understand the potential reasons for the observed activity among **1**, **4**, and **5**, these structures were geometrically optimized at the HF/6-31G** level of theory in Jaguar. We found that the N1 atom in **5** (Chart 1) prefers a pyramidal configuration instead of a planar one even though it is planar when optimized at a lower level of theory (e.g., HF/3-21G). Similar nitrogen pyramidization was also observed in other systems experimentally[28] and in theoretical calculations.[29] With these optimized structures, we then generated molecular electrostatic potential (MEP) surface for each molecule from their respective electron densities (Figure 2). The major

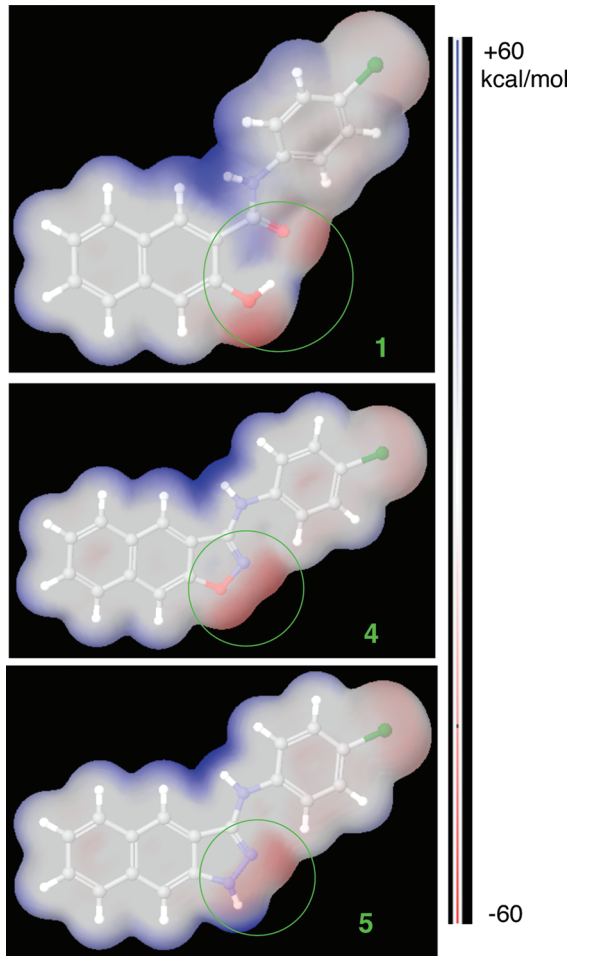

Figure 2. Molecular electrostatic potential (MEP) surfaces of **1**, **4**, and **5** mapped to their electron densities calculated at the HF/6-31G** level of theory in Jaguar. The blue indicates electrostatically positively charged regions, while the red is negatively charged. All the surfaces are normalized from −60 to +60 kcal/mol.

difference observed among **1**, **4**, and **5** is located in the linkage section as highlighted in green circles in Figure 2. In both of the active compounds **1** and **5**, this area is represented by positively and negatively charges surfaces. However, only electrostatically negatively charged (−40 to −50 kcal/mol) surfaces are present in the corresponding area in the inactive **4** (Figure 2). It could be that the binding site in KIX for the circled area is electrostatically negatively charged. As a consequence, **4** does not fit well in that binding site, contributing to its loss of inhibition of KIX−KID interaction. On the other hand, the mixed surfaces from **1** and **5** are well accommodated.

CONCLUSION

A series of compounds (**2**−**7**) were designed and synthesized to mimic two alternative conformations of **1** to derive its potential bioactive conformation in inhibiting KIX−KID interaction. These compounds were then biologically evaluated

dx.doi.org/10.1021/jm300043c | *J. Med. Chem.* 2012, 55, 4020−4024

for their capability to inhibit KIX−KID interaction in vitro and CREB-mediated gene transcription in HEK 293T cells. These results suggest that the energetically favored conformer **1b** may represent the bioactive conformation. Molecular modeling studies suggest that the electrostatic potential surface of the newly created heterocycle needs to be at least partially positively charged. Further investigations are underway to utilize these concepts to design more potent derivatives in inhibiting KIX−KID interaction and CREB-mediated gene transcription.

EXPERIMENTAL SECTION

General. See Supporting Information for details. All final compounds were confirmed to be of >95% purity based on HPLC analysis.

3-(4-Chlorophenyl)-2*H*-naphtho[2,3-*e*][1,3]oxazine-2,4-(3*H*)-dione (2). Compound **1** (100 mg, 0.34 mmol) was dissolved in *p*-xylene (4.0 mL), and the solution was stirred for 5 min at room temperature. Oxalyl chloride (150 μL, 1.7 mmol) in *p*-xylene (1.0 mL) was then added, and the mixture was heated at 120 °C overnight. The reaction mixture was cooled to room temperature. The precipitate was collected by filtration and washed with *p*-xylene to give a pink-white solid **17** (57 mg, 52%): mp 306−308 °C (dec). ^{1}H NMR (400 MHz, $CDCl_3$) δ 8.77 (s, 1 H), 8.06 (d, *J* = 8.4 Hz, 1 H), 7.96 (d, *J* = 8.4 Hz, 1 H), 7.78 (s, 1 H), 7.72 (t, *J* = 9.6 Hz, 1 H), 7.61 (t, *J* = 7.3 Hz, 1 H), 7.55 (d, *J* = 8.8 Hz, 2 H), 7.33 (d, *J* = 8.4 Hz, 2 H); ^{13}C NMR (100 MHz, DMSO-d_6) δ 161.3, 148.5, 148.1, 137.0, 134.8, 133.9, 131.1, 130.3, 130.1, 130.1, 129.6, 127.9, 126.9, 114.9, 112.6.

3-(4-Chlorophenyl)benzo[*g*]quinazoline-2,4-(1*H*,3*H*)-dione (3). Triphosgene (7.5 mg, 0.025 mmol) was added to a stirred solution of **11** (15 mg, 0.05 mmol) in THF (1.5 mL) at room temperature. The resulting mixture was heated under reflux for 2 h. The mixture was then cooled to room temperature and diluted with THF (5 mL). The solid was collected by filtration to give a white solid (11 mg, 69%): mp >400 °C. ^{1}H NMR (400 MHz, DMSO-d_6) δ 11.67 (s, 1 H), 8.70 (s, 1 H), 8.14 (d, *J* = 7.5 Hz, 1 H), 7.95 (d, *J* = 7.7 Hz, 1 H), 7.63 (dt, *J* = 7.5, 1.3 Hz, 1 H), 7.59 (s, 1 H), 7.57 (d, *J* = 9.0 Hz, 2 H), 7.47 (dt, *J* = 7.6, 1.3 Hz, 1 H), 7.43 (d, *J* = 8.8 Hz, 2 H); ^{13}C NMR (100 MHz, DMSO-d_6) δ 162.2, 150.1, 136.39, 135.41, 134.7, 132.7, 131.2, 129.6, 129.6, 129.4, 128.8, 128.5, 126.7, 125.0, 115.1, 110.1; ESI-MS *m*/*z* 320.7 $(M - H)^-$; HRESI-MS for $C_{18}H_{11}ClN_2O_2$ − H, calcd 321.0425, found 321.0416.

***N*-(4-Chlorophenyl)naphtho[2,3-*d*]isoxazol-3-amine (4).** K_2CO_3 (7.9 mg, 0.057 mmol) was added to a stirred solution of **22** (6.0 mg, 0.019 mmol) in DMF (1 mL) at room temperature. The resulting mixture was then heated at 110 °C for 4 h. The mixture was cooled to room temperature, and DMF was removed in vacuo. The residue was dissolved in EtOAc (50 mL), which was then washed with H_2O (2 × 10 mL) and brine (2 × 10 mL). The organic solution was dried over anhydrous Na_2SO_4, filtered, and concentrated. The residue was then subjected to column chromatography, eluting with hexanes/EtOAc (10:1 to 4:1) to give a white solid (2.7 mg, 48%): mp 218−220 °C. ^{1}H NMR (400 MHz, $CDCl_3$) δ 8.12 (s, 1 H), 7.98 (d, *J* = 8.8 Hz, 1 H), 7.95 (d, *J* = 8.4 Hz, 1 H), 7.86 (s, 1 H), 7.60 (d, *J* = 8.8 Hz, 2 H), 7.56 (td, *J* = 8.4, 1.2 Hz, 1 H), 7.47 (td, *J* = 8.0, 1.2 Hz, 1 H), 7.35 (d, *J* = 8.8 Hz, 2 H), 6.60 (brs, 1 H); ESI-MS *m*/*z* 295 $(M + H)^+$; HRESI-MS for $C_{17}H_{11}ClN_2O$ − H, calcd 293.0476, found 293.0470.

***N*-(4-Chlorophenyl)-1*H*-benzo[*f*]indazol-3-amine (5).** A mixture of thioamide **24** (60 mg, 0.19 mmol) in anhydrous hydrazine/DMSO (0.5/0.5 mL) was stirred at 150 °C for 1 h. The mixture was cooled to room temperature and poured into water (10 mL). The organic compound was extracted with dichloromethane (3 × 10 mL). The combined organic layers were washed with brine (2 × 10 mL), dried with Na_2SO_4, filtered, and concentrated. The residue was purified by silica gel flash column chromatography, eluting with hexanes/ethyl acetate (4:1) to yield a yellow solid (10 mg, 18%): mp 220−221 °C. ^{1}H NMR (400 MHz, DMSO-d_6) δ 11.95 (s, 1 H), 9.37 (s, 1 H), 8.62 (s, 1 H), 7.98 (d, *J* = 8.0 Hz, 1 H), 7.96 (d, *J* = 8.0 Hz, 1 H), 7.82 (s, 1 H), 7.81 (d, *J* = 8.8 Hz, 2 H), 7.44 (t, *J* = 8.0 Hz, 1 H), 7.34 (d, *J* = 8.8 Hz, 2 H), 7.32 (t, *J* = 8.4 Hz, 1 H); ^{13}C NMR (100 MHz, DMSO-d_6) δ 145.2, 142.1, 139.9, 133.3, 129.5, 129.0, 127.9, 127.5, 126.3, 123.0, 122.9, 119.1, 117.9, 104.3; ESI-MS *m*/*z* 292 $(M - H)^-$; HRESI-MS for $C_{17}H_{12}ClN_3$ − H, calcd 292.0636, found 292.0629.

***N*-(4-Chlorophenyl)-1-methyl-1*H*-benzo[*f*]indazol-3-amine (6).** NaH (60% in mineral oil, 6 mg, 0.15 mmol) was added to a stirred solution of **5** (40 mg, 0.136 mmol) in DMF (0.5 mL) at 0 °C under Ar. The mixture was stirred at 0 °C for 30 min, when CH_3I (8.6 μL, 0.136 mmol) was added. The mixture was stirred at room temperature for another 1 h and poured into cooled water (10 mL). The precipitate was collected by filtration. The yellow solid was purified by silica gel flash column chromatography, eluting with hexanes/ethyl acetate, 4:1, to yield a yellow solid (19 mg, 45%): mp 121−122 °C. ^{1}H NMR (400 MHz, DMSO-d_6) δ 9.47 (s, 1 H), 8.64 (s, 1 H), 8.00 (d, *J* = 8.8 Hz, 1 H), 7.96 (d, *J* = 8.4 Hz, 1 H), 7.91 (s, 1 H), 7.83 (d, *J* = 8.8 Hz, 2 H), 7.54 (t, *J* = 8.4 Hz, 1 H), 7.37 (d, *J* = 8.8 Hz, 2 H), 7.32 (t, *J* = 8.0 Hz, 1 H), 3.98 (s, 3 H); ^{13}C NMR (100 MHz, DMSO-d_6) δ 143.8, 141.3, 139.3, 132.9, 129.1, 128.6, 127.3, 126.9, 126.1, 122.7, 122.6, 119.1, 117.7, 117.5, 103.1, 35.3; ESI-MS *m*/*z* 305.9 $(M - H)^-$; HRESI-MS for $C_{18}H_{14}ClN_3$ − H, calcd 306.0793, found 306.0785.

***N*-(4-Chlorophenyl)benzo[*g*]quinazolin-4-amine (7).** A mixture of 4-chlorobenzo[*g*]quinazoline (**27**) (50 mg, 0.23 mmol), 4-chloroaniline (36 mg, 0.28 mmol), and DMAP (29 mg, 0.23 mmol) in *p*-xylene (1 mL) was stirred at 140 °C for 10 min. The mixture was cooled to room temperature. Evaporation of *p*-xylene resulted in a residue which was subjected to silica gel flash column chromatography, eluting with hexanes/ethyl acetate (2:1) to yield a yellow solid (31 mg, 44%): mp 251−252 °C. ^{1}H NMR (400 MHz, $CDCl_3$) δ 10.26 (s, 1 H), 9.32 (s, 1 H), 8.67 (s, 1 H), 8.47 (s, 1 H), 8.21 (d, *J* = 8.8 Hz, 1 H), 8.19 (d, *J* = 8.4 Hz, 1 H), 8.08 (d, *J* = 8.8 Hz, 2 H), 7.42 (t, *J* = 7.2 Hz, 1 H), 7.67 (t, *J* = 7.2 Hz, 1 H), 7.54 (d, *J* = 8.8 Hz, 2 H); ^{13}C NMR (100 MHz, $CDCl_3$) δ 158.6, 154.4, 145.5, 138.6, 135.9, 131.4, 129.3, 128.9, 128.5, 128.3, 128.0, 126.8, 125.5, 124.3, 123.7, 115.5; ESI-MS *m*/*z* 303.9 $(M - H)^-$; HRESI-MS for $C_{18}H_{12}ClN_3$ + H, calcd 306.0793, found 306.0805.

ASSOCIATED CONTENT

Supporting Information

Experimental procedures for synthesis of and characterization data for **9**−**11**, **19**−**20**, and **22**−**27**; details of the biological assays and molecular modeling. This material is available free of charge via the Internet at http://pubs.acs.org.

AUTHOR INFORMATION

Corresponding Author

*Phone: 503-494-4748. Fax: 503-494-4352. E-mail: xiaoxi@ohsu.edu.

Notes

The authors declare no competing financial interest.

ACKNOWLEDGMENTS

This work was made possible by financial support from NIH (Grant R01GM087305) and Susan G. Komen for the Cure (Grant KG100458). We thank Jenny Luo, Dr. Andrea DeBarber, and Dr. Dennis Koop for running the mass spectroscopic analyses.

ABBREVIATIONS USED

CRE, cyclic AMP response element; CREB, cyclic AMP response element binding protein; CBP, CREB-binding protein; KID, kinase-inducible domain; KIX, kinase-inducible domain interacting; p-CREB, phosphorylated cyclic AMP response element binding protein; PKA, protein kinase A; PKB, protein kinase B; MAPK, mitogen-activated protein kinase; pp90^{RSK}, protein p90 ribosomal S6 kinase; NSCLC,

non-small-cell lung cancer; NOE, nuclear Overhauser effect; MEP, molecular electrostatic potential; S_NAr, nucleophilic aromatic substitution

REFERENCES

(1) Shaywitz, A. J.; Greenberg, M. E. CREB: a stimulus-induced transcription factor activated by a diverse array of extracellular signals. *Annu. Rev. Biochem.* **1999**, *68*, 821−861.

(2) Montminy, M. R.; Bilezikjian, L. M. Binding of a nuclear-protein to the cyclic-AMP response element of the somatostatin gene. *Nature* **1987**, *328*, 175−178.

(3) Montminy, M. R.; Sevarino, K. A.; Wagner, J. A.; Mandel, G.; Goodman, R. H. Identification of a cyclic-AMP-responsive element within the rat somatostatin gene. *Proc. Natl. Acad. Sci. U.S.A.* **1986**, *83*, 6682−6686.

(4) Gonzalez, G. A.; Montminy, M. R. Cyclic AMP stimulates somatostatin gene transcription by phosphorylation of CREB at serine 133. *Cell* **1989**, *59*, 675−680.

(5) Radhakrishnan, I.; PerezAlvarado, G. C.; Parker, D.; Dyson, H. J.; Montminy, M. R.; Wright, P. E. Solution structure of the KIX domain of CBP bound to the transactivation domain of CREB: Aa model for activator:coactivator interactions. *Cell* **1997**, *91*, 741−752.

(6) Du, K. Y.; Montminy, M. CREB is a regulatory target for the protein kinase Akt/PKB. *J. Biol. Chem.* **1998**, *273*, 32377−32379.

(7) Xing, J.; Ginty, D. D.; Greenberg, M. E. Coupling of the RAS-MAPK pathway to gene activation by RSK2, a growth factor-regulated CREB kinase. *Science* **1996**, *273*, 959−963.

(8) Tan, Y.; Rouse, J.; Zhang, A. H.; Cariati, S.; Cohen, P.; Comb, M. J. FGF and stress regulate CREB and ATF-1 via a pathway involving p38 MAP kinase and MAPKAP kinase-2. *EMBO J.* **1996**, *15*, 4629−4642.

(9) Ginty, D. D.; Bonni, A.; Greenberg, M. E. Nerve growth factor activates a Ras-dependent protein kinase that stimulates c-fos transcription via phosphorylation of CREB. *Cell* **1994**, *77*, 713−725.

(10) Seo, H. S.; Liu, D. D.; Bekele, B. N.; Kim, M. K.; Pisters, K.; Lippman, S. M.; Wistuba, I. I.; Koo, J. S. Cyclic AMP response element-binding protein overexpression: a feature associated with negative prognosis in never smokers with non-small cell lung cancer. *Cancer Res.* **2008**, *68*, 6065−6073.

(11) Wu, W.; Zhau, H. E.; Huang, W. C.; Iqbal, S.; Habib, F. K.; Sartor, O.; Cvitanovic, L.; Marshall, F. F.; Xu, Z.; Chung, L. W. K. cAMP-responsive element-binding protein regulates vascular endothelial growth factor expression: implication in human prostate cancer bone metastasis. *Oncogene* **2007**, *26*, 5070−5077.

(12) Chhabra, A.; Fernando, H.; Watkins, G.; Mansel, R. E.; Jiang, W. G. Expression of transcription factor CREB1 in human breast cancer and its correlation with prognosis. *Oncol. Rep.* **2007**, *18*, 953−958.

(13) Crans-Vargas, H. N.; Landaw, E. M.; Bhatia, S.; Sandusky, G.; Moore, T. B.; Sakamoto, K. M. Expression of cyclic adenosine monophosphate response-element binding protein in acute leukemia. *Blood* **2002**, *99*, 2617−2619.

(14) Shankar, D. B.; Cheng, J. C.; Kinjo, K.; Federman, N.; Moore, T. B.; Gill, A.; Rao, N. P.; Landaw, E. M.; Sakamoto, K. M. The role of CREB as a proto-oncogene in hematopoiesis and in acute myeloid leukemia. *Cancer Cell* **2005**, *7*, 351−362.

(15) Xiao, X.; Li, B. X.; Mitton, B.; Ikeda, A.; Sakamoto, K. M. Targeting CREB for cancer therapy: friend or foe. *Curr. Cancer Drug Targets* **2010**, *10*, 384−391.

(16) Aggarwal, S.; Kim, S. W.; Ryu, S. H.; Chung, W. C.; Koo, J. S. Growth suppression of lung cancer cells by targeting cyclic AMP response element-binding protein. *Cancer Res.* **2008**, *68*, 981−988.

(17) Best, J. L.; Amezcua, C. A.; Mayr, B.; Flechner, L.; Murawsky, C. M.; Emerson, B.; Zor, T.; Gardner, K. H.; Montminy, M. Identification of small-molecule antagonists that inhibit an activator:coactivator interaction. *Proc. Natl. Acad. Sci. U.S.A.* **2004**, *101*, 17622−17627.

(18) Li, B. X.; Xiao, X. Discovery of a small-molecule inhibitor of the KIX−KID interaction. *ChemBioChem* **2009**, *10*, 2721−2724.

(19) Mu, F.; Lee, D. J.; Pryor, D. E.; Hamel, E.; Cushman, M. Synthesis and investigation of conformationally restricted analogues of lavendustin A as cytotoxic inhibitors of tubulin polymerization. *J. Med. Chem.* **2002**, *45*, 4774−4785.

(20) Yevich, J. P.; New, J. S.; Smith, D. W.; Lobeck, W. G.; Catt, J. D.; Minielli, J. L.; Eison, M. S.; Taylor, D. P.; Riblet, L. A.; Temple, D. L., Jr. Synthesis and biological evaluation of 1-(1,2-benzisothiazol-3-yl)- and (1,2-benzisoxazol-3-yl)piperazine derivatives as potential antipsychotic agents. *J. Med. Chem.* **1986**, *29*, 359−369.

(21) Kalkote, U. R.; Goswami, D. D. New synthesis of 1,2-benzisoxazole derivatives. *Aust. J. Chem.* **1977**, *30*, 1847−1850.

(22) Yale, H. L. The hydroxamic acids. *Chem. Rev.* **1943**, *33*, 209−256.

(23) Deng, B. L.; Hartman, T. L.; Buckheit, R. W., Jr.; Pannecouque, C.; De Clercq, E.; Fanwick, P. E.; Cushman, M. Synthesis, anti-HIV activity, and metabolic stability of new alkenyldiarylmethane HIV-1 non-nucleoside reverse transcriptase inhibitors. *J. Med. Chem.* **2005**, *48*, 6140−6155.

(24) Shi, G. The first general synthesis of N-substituted 1,2-benzisoxazolin-3-ones. *Tetrahedron Lett.* **2000**, *41*, 2295−2298.

(25) Pettus, L. H.; Xu, S.; Cao, G.-Q.; Chakrabarti, P. P.; Rzasa, R. M.; Sham, K.; Wurz, R. P.; Zhang, D.; Middleton, S.; Henkle, B.; Plant, M. H.; Saris, C. J. M.; Sherman, L.; Wong, L. M.; Powers, D. A.; Tudor, Y.; Yu, V.; Lee, M. R.; Syed, R.; Hsieh, F.; Tasker, A. S. 3-Amino-7-phthalazinylbenzoisoxazoles as a novel class of potent, selective, and orally available inhibitors of p38α mitogen-activated protein kinase. *J. Med. Chem.* **2008**, *51*, 6280−6292.

(26) Burke, M. J.; Trantow, B. M. An efficient route to 3-aminoindazoles and 3-amino-7-azaindazoles. *Tetrahedron Lett.* **2008**, *49*, 4579−4581.

(27) Oerfi, L.; Waczek, F.; Pato, J.; Varga, I.; Hegymegi-Barakonyi, B.; Houghten, R. A.; Keri, G. Improved, high yield synthesis of 3*H*-quinazolin-4-ones, the key intermediates of recently developed drugs. *Curr. Med. Chem.* **2004**, *11*, 2549−2553.

(28) Acheson, R. M.; Benn, M. H.; Jacyno, J.; Wallis, J. D. Pyramidal bonding about nitrogen in 1-benzoyloxyindole determined by X-ray diffraction. *J. Chem. Soc., Perkin Trans. 2* **1983**, 497−500.

(29) Gould, I. R.; Kollman, P. A. Theoretical investigation of the hydrogen-bond strengths in guanine-cytosine and adenine-thymine base-pairs. *J. Am. Chem. Soc.* **1994**, *116*, 2493−2499.